Biaxial order in spin nematics

R. Haramoto and J. Sak
Serin Physics Laboratory, Rutgers University, Piscataway, New Jersey 08854-0849
(Received 6 January 1992)

We study a model of a spin nematic based on two spins $S_1=1$ and $S_2=1$ on each site. The couplings favor perpendicular configuration of S_1 to S_2 and parallel alignment of the S_1 and the S_2 spins, respectively. Four phases were found, including isotropic, two uniaxial, and a biaxial phase. The phase diagram is reminiscent of but different from liquid-crystal nematics.

Spin nematics are a class of quantum or classical spin models with biquadratic couplings, and have been studied for some time.[1] Interest in these models has broadened considerably because of possible connections with high-temperature superconductivity.[2,3]

Spin nematics may display orientational order at sufficiently low temperatures but the mutually opposite directions are equivalent, in analogy to liquid-crystal nematics.[4] The usual picture of a phase diagram of a liquid-crystal nematic contains first-order lines that separate the isotropic phase from uniaxial nematic phases (prolate and oblate.) The two uniaxial phases are separated by a biaxial region in which the system is anisotropic in all three directions. The boundary between uniaxial phases and the biaxial phase is a second-order transition. All four phases meet at a single point, sometimes called the Landau point (for reviews see Refs. 5 and 6). However, Allender and co-workers[7,8] studied Landau type phenomenological theories which for certain ranges of parameters yield phase diagrams that have shapes somewhat different from the standard picture, in particular, there are no points where all four phases meet.

In this short paper we would like to explore the similarities and differences between liquid-crystal nematics and spin nematics in more detail. Uniaxial phases, usually referred to as quadrupolar orderings, were already found by Andreev and Grishchuk[9] and by Buzano.[10] One of our purposes has been to find a model displaying a biaxial phase. To this end we place two spins $S_1=1$ and $S_2=1$ on each site of a lattice (the nature of the lattice is irrelevant, since we are going to use mean-field theory). There is a strong coupling $-G_3(\mathbf{S}_1\cdot\mathbf{S}_2)^2$, $G_3<0$ between the two spins on each site. This coupling favors a configuration that best approximates the classical limit in which $\mathbf{S}_1$ and $\mathbf{S}_2$ are perpendicular to each other. The two spins form a unit, a kind of "molecule." The molecules on different sites interact via two couplings

$$-g_1(\mathbf{S}_1\cdot\mathbf{S}_1)^2-g_2(\mathbf{S}_2\cdot\mathbf{S}_2)^2,\ g_1\geq g_2>0\ ,$$

which at sufficiently low temperatures, tend to align the $\mathbf{S}_1$ spins in some direction $\pm\mathbf{n}$ and, at still lower temperatures, the $\mathbf{S}_2$ spins will align along some direction $\pm\mathbf{m}$ in the plane perpendicular to $\pm\mathbf{n}$. The couplings g_1 and g_2 are constants and do not depend on the distance between the sites (mean-field assumption.)

The Hamiltonian describing this two-spin system is

$$H=-\sum_{a,b=1}^{N}[g_1(\mathbf{S}_{1a}\cdot\mathbf{S}_{1b})^2+g_2(\mathbf{S}_{2a}\cdot\mathbf{S}_{2b})^2 + G_3\delta_{ab}(\mathbf{S}_{1a}\cdot\mathbf{S}_{2a})^2]\ , \tag{1}$$

where the sum is over N lattice sites, and the spin-1 operators are given by

$$S^x=\frac{1}{\sqrt{2}}\begin{bmatrix}0&1&0\\1&0&1\\0&1&0\end{bmatrix}\ , \tag{2}$$

$$S^y=\frac{i}{\sqrt{2}}\begin{bmatrix}0&-1&0\\1&0&-1\\0&1&0\end{bmatrix}\ , \tag{3}$$

$$S^z=\begin{bmatrix}1&0&0\\0&0&0\\0&0&-1\end{bmatrix}\ . \tag{4}$$

We choose the basis that diagonalizes $S_1^z+S_2^z$ and $\mathbf{S}^2$, $\mathbf{S}=\mathbf{S}_1+\mathbf{S}_2$ (for the case of 2 spin 1/2's see Refs. 11 and 12).

The spin eigenfunctions with

$$|\mathbf{S}|=2\ \text{ and }\mathbf{S}_1\cdot\mathbf{S}_2=\tfrac{1}{2}S(S+1)-2=+1$$

are given by

$$|2,\pm2\rangle=|1,\pm1;1,\pm1\rangle\ , \tag{5}$$

$$|2,\pm1\rangle=\frac{1}{\sqrt{2}}(|1,\pm1;1,0\rangle+|1,0;1,\pm1\rangle)\ , \tag{6}$$

$$|2,0\rangle=\frac{1}{\sqrt{6}}(|1,1;1,-1\rangle+2|1,0;1,0\rangle+|1,-1;1,1\rangle)\ . \tag{7}$$

The next set of eigenfunctions with $|\mathbf{S}|=1$ and $\mathbf{S}_1\cdot\mathbf{S}_2=-1$ are energetically degenerate with the $|\mathbf{S}|=2$ states

$$|1,\pm1\rangle=\pm\frac{1}{\sqrt{2}}(|1,\pm1;1,0\rangle-|1,0;1,\pm1\rangle)\ , \tag{8}$$

$$|1,0\rangle=\frac{1}{\sqrt{2}}(|1,1;1,-1\rangle-|1,-1;1,1\rangle)\ . \tag{9}$$

The last spin eigenfunction, with $|\mathbf{S}|=0$ and $\mathbf{S}_1\cdot\mathbf{S}_2=-2$, is frozen out and does not affect the behavior of the system at low temperature when G_3 is large in absolute

value and negative

$$|0,0\rangle=\frac{1}{\sqrt{3}}(|1,1;1,-1\rangle-|1,0;1,0\rangle+|1,-1;1,1\rangle)\ . \tag{10}$$

To introduce the mean-field Hamiltonian we define

$$M_1^{ij}=\langle S_1^i S_1^j\rangle\ , \tag{11}$$

$$M_2^{ij}=\langle S_2^i S_2^j\rangle\ , \tag{12}$$

where the averages are defined by a self-consistency condition to be formulated presently. The mean-field Hamiltonian is now given by

$$H_{\rm MF}=-\left[\sum_{i,j=x,y,z} G_1 S_1^i S_1^j M_1^{ij}+\sum_{i,j=x,y,z} G_2 S_2^i S_2^j M_2^{ij}+G_3(\mathbf{S}_1\cdot\mathbf{S}_2)^2\right]\ , \tag{13}$$

where $G_1=Ng_1$, and $G_2=Ng_2$.

Now we close the system by defining the averages as

$$\langle\hat{O}\rangle=\frac{1}{Z}\sum_{p=1}^{9}\langle p|\hat{O}\exp(-\beta H_{\rm MF})|p\rangle\ , \tag{14}$$

where $\hat{O}$ is an arbitrary operator, $\beta=1/T$ is the inverse of the temperature, and the normalizing factor Z is the one-site partition function,

$$Z=\sum_{p=1}^{9}\langle p|\exp(-\beta H_{\rm MF})|p\rangle\ . \tag{15}$$

By choosing the coordinate system to coincide with the proper axis of the molecules, we set the off-diagonal elements to zero, leaving us with the six mean-field variables, M_1^{xx}, M_1^{yy}, M_1^{zz}, M_2^{xx}, M_2^{yy}, and M_2^{zz}.

We solve these equations numerically, using a self-consistent approach. First we calculate the matrix elements $\langle p|S_1^x S_1^x|q\rangle,\langle p|S_1^y S_1^y|q\rangle,\ldots,\langle p|S_2^z S_2^z|q\rangle,\langle p|(\mathbf{S}_1\cdot\mathbf{S}_2)^2|q\rangle$, where $p,q=1,\ldots,9$, then substitute into the symmetric Hamiltonian,

$$\langle p|H_{\rm MF}|q\rangle=-\left[G_1\sum_{i=x,y,z}\langle p|S_1^i S_1^i|q\rangle M_1^{ii}+G_2\sum_{i=x,y,z}\langle p|S_2^i S_2^i|q\rangle M_2^{ii}+G_3\langle p|(\mathbf{S}_1\cdot\mathbf{S}_2)^2|q\rangle\right]\ . \tag{16}$$

Choosing suitable initial values for our mean-field variables we compute the Hamiltonian, invoke the standard (EISPACK) routines[13,14] to find the eigenvalues and eigenvectors, then compute the mean-field variables

$$M_1^{ii}=\frac{1}{Z}\sum_{pqrsvw=1}^{9}U_{pq}^{\dagger}\langle q|S_1^i S_1^i|r\rangle U_{rs}U_{sv}^{\dagger}\langle v|\exp(-\beta H_{\rm MF})|w\rangle U_{wp}\ , \tag{17}$$

$$M_2^{ii}=\frac{1}{Z}\sum_{pqrsvw=1}^{9}U_{pq}^{\dagger}\langle q|S_2^i S_2^i|r\rangle U_{rs}U_{sv}^{\dagger}\langle v|\exp(-\beta H_{\rm MF})|w\rangle U_{wp}\ , \tag{18}$$

where $i=x,y,z$, and U is the normalized matrix of eigenvectors of $H_{\rm MF}$. If we let E_p be the energy eigenvalue corresponding to the pth eigenvector, then we find

$$\sum_{v,w=1}^{9}U_{sv}^{\dagger}\langle v|\exp(-\beta H_{\rm MF})|w\rangle U_{wp}=\delta_{sp}\exp(-\beta E_p)\ , \tag{19}$$

so that the expectation values for the mean-field variables simplifies to a rotation and a trace weighted by a Boltzmann factor.

If just one of the new expectation values differs from its previous value by more than 10^{-8}, the calculation is repeated, the new expectation values are substituted into the Hamiltonian and another set of eigenvalues and eigenvectors are calculated. This process is continued until the mean-field variables converge to a stable solution.

After we have found the solution, we plot the following order-parameter functions

$$Q_{1xx}=\langle S_1^x S_1^x\rangle-\tfrac{1}{3}\langle\mathbf{S}_1\cdot\mathbf{S}_1\rangle\ , \tag{20}$$

$$Q_{2xx}=\langle S_2^x S_2^x\rangle-\tfrac{1}{3}\langle\mathbf{S}_2\cdot\mathbf{S}_2\rangle\ . \tag{21}$$

The Q_{1yy}, Q_{1zz}, Q_{2yy}, and Q_{2zz} are defined analogously. The identity $M_1^{xx}+M_1^{yy}+M_1^{zz}=2$ is used as a check on the accuracy of the numerical calculations. In addition the results $\langle\mathbf{S}_1\rangle=\mathbf{0}$ and $\langle\mathbf{S}_2\rangle=\mathbf{0}$, indicate that we have quadrupolar ordering in the uniaxial and biaxial phases and no dipolar order.

The following symmetry can be exploited. In finding the lines of the phase diagram we can limit the values of G_2 to the region $G_2<G_1$. We find that the transition temperatures are related for different G_2's, given by the expressions $T'=(G_1/G_2)T$ when $G_1'=G_1, G_2'=G_1^2/G_2$ and $G_3'=(G_1/G_2)G_3$. When the parameters were accurate to 10^{-9}, our model produced a transition temperature that agreed with the predicted conjugate transition temperature to eight decimal places.

However, for the case of large and negative G_3, the states $|\mathbf{S}|=0$ are frozen out, and since the $|\mathbf{S}|=1$ and $|\mathbf{S}|=2$ states both have equal single-site energies of $-G_3$, we see that G_3 should not affect the transition tempera-

ture. When $G_1=7$ and $G_3=-10$, we find that $G_2=10$ is conjugate to $G_2=4.9$ and the transition temperatures differ from the predicted conjugate temperatures by less than 0.3%. The agreement between conjugate temperatures is even better for $G_1=7$ and $G_3=-50$, comparing $G_2=10$ and its conjugate $G_2=4.9$, we see that the transition temperatures differ from the predicted conjugate temperatures by less than 0.07%. For fixed values of G_1 and G_2, an 80% drop in the magnitude of $G_3=-50$ caused the transition temperatures to change by less than 1%. To estimate when G_3 is "large," we compare the single-site energy factors that contribute to the partition function. When $G_3=-1$, and taking the transition temperature to be of the order of $T=2$, we find

$$\exp(\beta G_3\langle |\mathbf{S}|=1 \text{ or } 2|(\mathbf{S}_1\cdot\mathbf{S}_2)^2||\mathbf{S}|=1 \text{ or } 2\rangle)=\exp(\beta G_3)$$

is the same order of magnitude as

$$\exp(\beta G_3\langle 0|(\mathbf{S}_1\cdot\mathbf{S}_2)^2|0\rangle)=\exp(4\beta G_3)\ .$$

When $G_3=-10$, $\exp(4\beta G_3)$ is over a million times smaller than $\exp(\beta G_3)$, and for $G_3=-50$, $\exp(4\beta G_3)$ is smaller than $\exp(\beta G_3)$ by 32 orders of magnitude. Therefore we can safely ignore the effects of G_3 on the transition temperature when $G_3\le -10$.

The phase diagram was computed by selecting a value of G_2 and examining the order-parameter functions versus temperature. In order to locate the transition temperatures we divide the temperature axis into decades, we start out with some temperature and examine the ten increments spaced by ΔT, the transition temperatures were identified manually at a precision of ΔT, then the program was run over again with the change in temperature ΔT smaller by a factor of 10. First-order transitions were fairly quick to converge, usually less than 10^4 iterations, while second-order transitions took as much as 100 times longer when $\Delta T=10^{-5}$. Since higher accuracy was not required for our phase diagrams, smaller ΔT values were used for only a select number of points.

The phase diagram shown in Fig. 1 has a first-order transition from the isotropic phase to the uniaxial phase. We find a fairly broad range of values of G_2 where the system undergoes a first-order transition from the isotropic phase to the biaxial phase, the sharpness of the transition decreases slightly as G_2 moves away from G_1 (Fig. 2 shows the behavior of the order parameters when G_2 is near the end of the line of isotropic-to-biaxial phase transitions).

The line of uniaxial-to-biaxial phase transitions is first order for the observed values of G_2 and for G_3 in the range $-0.1\le G_3\le 0$. As G_3 gets stronger this transition weakens considerably, and, as shown in Fig. 3, for $G_1=7$, $G_2=6$, $G_3=-10$, there is a second-order transition. The jump in Q_{2zz} and $(\Delta Q_{2zz})^2$ is shown in Fig. 4. The square of the jump in Q_{2zz} is a straight line that intersects the axis at $G_2=6.38$; we identify this value to be the tricritical point dividing the two types of transitions.

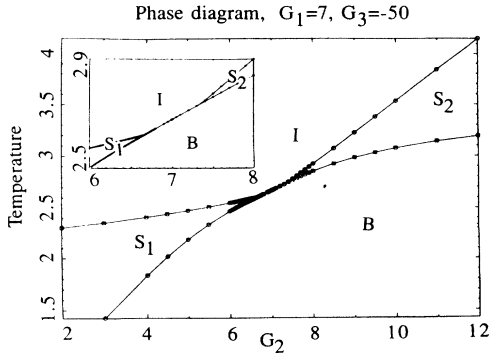

FIG. 1. Phase diagram for $G_1=7$, $G_3=-50$ displays an isotropic (I) phase, alignment of only spin-1 (S_1), alignment of only spin-2 (S_2), and a biaxial phase (B). The isotropic-to-uniaxial and isotropic-to-biaxial phase transitions are first order, while the uniaxial-to-biaxial phase transitions are second order from $G_2=3$ to about $G_2=6.1$, and first order from $6.1\le G_2\le 6.7$. The inset shows the central portion of the diagram in detail.

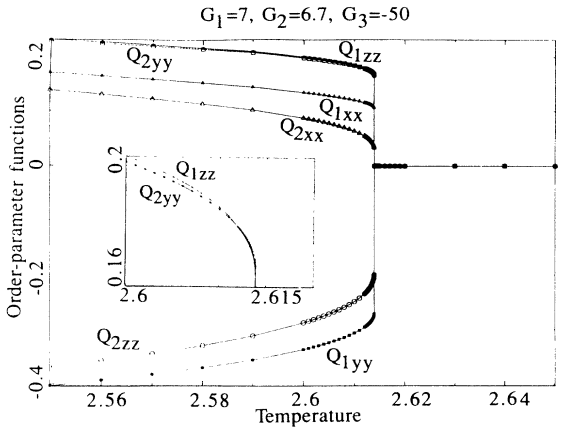

FIG. 2. Order parameter functions for $G_1=7$, $G_2=6.7$, $G_3=-50$. Solid points are the S_1 order parameter functions, the open points belong to S_2 order parameter, and $\Delta T=10^{-6}$ near the transition point. The inset is an expanded view of Q_{1zz} and Q_{2yy}.

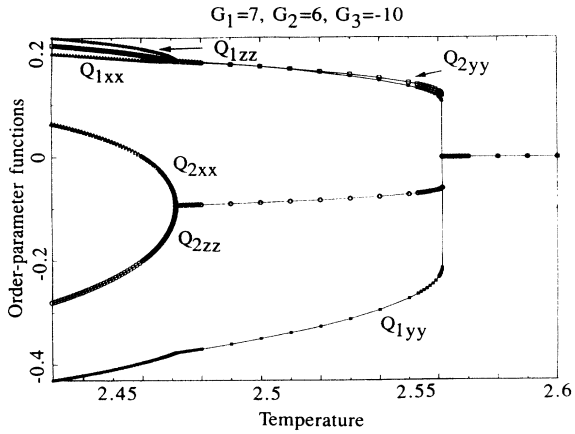

FIG. 3. Order parameter functions for $G_1=7$, $G_2=6, G_3=-10$. The solid points correspond to the S_1 order parameter and the open points are the S_2 order parameter functions; $\Delta T=10^{-6}$ near the transition points. Note that when one spin aligns, G_3 induces alignment in the other spin.

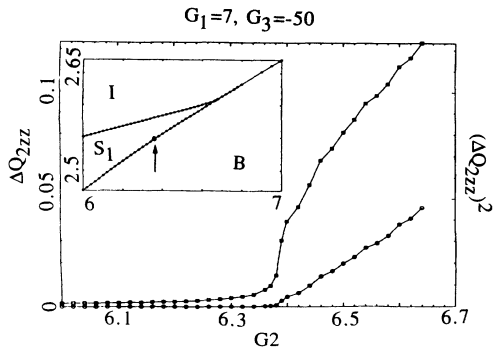

FIG. 4. The top curve is the discontinuity in Q_{2zz} at the line of uniaxial-biaxial transitions. The lower curve is the square of the jump in Q_{2zz}. The lower curve is nearly a straight line that intersects the axis around 6.38. We take this value to be an estimate for the tricritical point. The inset shows the location on the phase diagram. The arrow points to the tricritical point.

The inset in Fig. 4 displays an expanded view of the phase diagram, and indicates the location of the tricritical point.

Even for values of G_3 as small as $G_3 = -0.2$, where the isotropic $|\mathbf{S}| = 0$ state contributes substantially to the expectation values, we observed a line of second-order uniaxial-to-biaxial phase transitions meeting a line of first-order uniaxial-to-biaxial phase transitions. This seems to be a fairly robust feature of the model that is not dependent on the suppression of the $|\mathbf{S}| = 0$ state.

We would like to compare the phase diagram of our model with those for nematic liquid crystals.[6–8,15–18] The latter are obtained from mean-field theories of interacting anisotropic particles (ellipsoids) or from phenomenological theories of the Landau type. With the exception of Ref. 8, they are all characterized by the presence of a multicritical point at which all phases meet. In particular all mean-field models yield diagrams of such topology. However, Allender, Lee, and Hafiz[8] studied a Landau-type theory of a very general kind (11 parameters) and showed that in a certain range of the parameters the multicritical point is replaced by a curvilinear segment of first-order transitions where the isotropic and biaxial phases meet, just as in our model. The uniaxial-biaxial transitions are not described in sufficient detail in Ref. 8, specifically, it is not clear if there exist two tricritical points dividing the uniaxial-biaxial lines as we found in our model of a spin nematic. The theory of Allender, Lee, and Hafiz contains a large number of parameters and it is not unexpected that a wide variety of phase diagrams are consistent with it. On the other hand, our model is very simple: it contains three coupling constants, of which only two ratios matter and thus is more reminiscent of classical infinite range interaction models. It is perhaps surprising that we obtained a diagram that is qualitatively different from all the other ones based on microscopic models.

Finally, we wish to comment on the assumption of infinite range interactions. Such an assumption has the effect of suppressing fluctuations. The question arises, to what extent could our conclusion change in a more realistic theory, which takes fluctuations into account. We can offer a general argument that the central portion of the phase diagram (consisting of the first order I-B line and first-order portions of the B-S_1 and B-S_2 lines) will be qualitatively unaffected by fluctuation. Since the first-order transition takes place between two metastable states, the fluctuations, while in general not negligible, are nevertheless not catastrophic as is the case for the second-order transition. This gives us reason to believe that the first-order transitions will remain qualitatively unchanged even when fluctuations are included.

[1]E. L. Nagaev, Usp. Fiz. Nauk **138**, 61 (1982) [Sov. Phys. Usp. **25**, 31 (1982)].
[2]P. Chandra, P. Coleman, and I. Ritchey, J. Appl. Phys. **69**, 4974 (1991).
[3]V. Barzykin, L. P. Gor'kov, and A. V. Sokol, Europhys. Lett. **15**, 869 (1991).
[4]P. G. de Gennes, *The Physics of Liquid Crystals* (Clarendon, Oxford, 1974).
[5]Y. Galerne, Mol. Cryst. Liq. Cryst. **165**, 131 (1988).
[6]E. F. Gramsbergen, L. Longa, and W. H. de Jeu, Phys. Rep. **135**, 195 (1986).
[7]D. W. Allender and M. A. Lee, Mol. Cryst. Liq. Cryst. **110**, 331 (1984).
[8]D. W. Allender, M. A. Lee, and N. Hafiz, Mol. Cryst. Liq. Cryst. **124**, 45 (1985).
[9]A. F. Andreev and I. A. Grishchuk, Zh. Eksp. Teor. Fiz. **87**, 467 (1984) [Sov. Phys. JETP **60**, 267 (1984)].
[10]C. Buzano, Phys. Scr. **37**, 573 (1987).
[11]S. Flugge, *Practical Quantum Mechanics II* (Springer-Verlag, Berlin, 1971).
[12]J. L. Cadorin and W. Figueiredo, Phys. Status Solidi B **153**, K73 (1989).
[13]W. H. Press, B. P. Flannery, S. A. Teukolsky, and W. T. Vetterling, *Numerical Recipes in C* (Cambridge University Press, Cambridge, 1988).
[14]B. T. Smith, J. M. Boyle, J. J. Dongarra, B. S. Garbow, Y. Ikebe, V. C. Klema, and C. B. Moler, *Matrix Eigensystem Routines - EISPACK Guide*, 2nd ed. (Springer-Verlag, Berlin, 1976), Vol. 6.
[15]M. J. Freiser, Mol. Cryst. Liq. Cryst. **14**, 165 (1971).
[16]R. Alben, Phys. Rev. Lett. **30**, 778 (1973).
[17]J. P. Straley, Phys. Rev. A **10**, 1881 (1974).
[18]N. Boccara, R. Mejdani, and L. De Seze, J. Phys. (Paris) **38**, 149 (1977).